



PAPER

## The birth of radiation

To cite this article: John Lekner 2019 *Eur. J. Phys.* **40** 025201

View the [article online](#) for updates and enhancements.



**IOP | ebooks**<sup>TM</sup>

Bringing you innovative digital publishing with leading voices to create your essential collection of books in STEM research.

Start exploring the collection - download the first chapter of every title for free.

# The birth of radiation

John Lekner 

School of Chemical and Physical Sciences, Victoria University of Wellington, PO Box 600, Wellington, New Zealand

E-mail: [john.lekner@vuw.ac.nz](mailto:john.lekner@vuw.ac.nz)

Received 13 November 2018, revised 13 December 2018

Accepted for publication 16 January 2019

Published 11 February 2019



CrossMark

## Abstract

The topology of electric field lines in electric dipole radiation of angular frequency  $\omega$  changes during each cycle. From the beginning of each cycle to the time  $t_c$  given by  $\omega t_c = \sqrt{2} - \arctan(\sqrt{2} - 1/\sqrt{2}) \approx 0.8$  there is no reconnection of field lines. In the time interval  $t = t_c$  to  $t = 1/\omega$  electric field lines separate from the charges on the dipole and close on themselves, but the closed loops eventually die away. For times  $t = 1/\omega$  to  $t = \pi/2\omega$  the closed loops do not fade away but fly off to infinity as radiation. This sequence is repeated twice per cycle, with field direction reversal in the second half-cycle.

Keywords: radiation, dipole, field line topology

(Some figures may appear in colour only in the online journal)

Many authors, beginning with Hertz, have discussed and sometimes illustrated the transition in dipole radiation from bound fields, with electric field lines originating and ending on charges, to free fields in which the electric field lines close on themselves [1–13]. (Papers [14–17] deal with related aspects of field lines.) Hertz describes the phenomenon as ‘a tendency of [field lines] to contract together; as this inflection contracts nearer and nearer ... a portion of each of the outer lines of force detaches itself into a self-closed line of force which advances independently into space...’. A specific time in the cycle at which this occurs was estimated by Zangwill [11], who characterizes the birth of radiation as ‘a topological process called *field line reconnection*’. This note builds on his section 20.5.2, of the same title, but finds agreement with the description given by Lorrain and Corson [4] and Good [7]: there is a time *interval* during which radiation is born, not one event per half-cycle. The beginning of this birth interval is at  $\omega t = 1$ , the end at  $\omega t = \pi/2$ .

Most of what follows is not new. The contributions of Hertz [1], Lorrain and Corson [4], Good [7] and Zangwill [11] have already been mentioned. Bitter [2] gives a physical description, in terms of electric and magnetic fields and the Poynting vector, of the breaking away of loops of electric field. Derby and Olbert [10] stress the key importance of ‘singular points’ (field zeros) where topological changes can occur. Technically, the only new result is

(9), which gives the constant in the equation for the field lines. However, this equation enables the topological critical points of dipole radiation to be located precisely. Analytical results are obtained, valid at all times during the first half-cycle (the second half is the same with field directions reversed). All the transitions in electric dipole radiation can thus be located exactly, from no detachment of field loops, to detachment but evanescence of field loops, to the radiation interval during which field loops detach and fly off to infinity. The content is suitable for graduate or senior undergraduate electromagnetism courses.

We shall examine the details of the simplest possible case, that of radiation from a point electric dipole oscillating at a fixed frequency. Suppose a dipole at the origin oscillates at angular frequency  $\omega = ck$  along the  $z$  axis:  $\mathbf{p} = \hat{\mathbf{z}} p_0 \cos \omega t$ . The electric and magnetic fields at distance  $r$  and polar angle  $\theta$  are (we omit the multiplier  $p_0 k^3$  in Gaussian units or  $(\mu_0/4\pi)p_0 k^3$  in SI units)

$$\begin{aligned} \mathbf{E} = & \hat{\mathbf{r}} \cos \theta 2(kr)^{-3} [\cos(kr - \omega t) + kr \sin(kr - \omega t)] \\ & + \hat{\boldsymbol{\theta}} \sin \theta (kr)^{-3} [\cos(kr - \omega t) + kr \sin(kr - \omega t)] \\ & - (kr)^2 \cos(kr - \omega t) \end{aligned} \quad (1)$$

$$\mathbf{B} = \hat{\boldsymbol{\phi}} \sin \theta (kr)^{-2} [\sin(kr - \omega t) - kr \cos(kr - \omega t)]. \quad (2)$$

These fields follow from the vector potential  $\mathbf{A} = k\mathbf{p}r^{-1} \sin(kr - \omega t)$  (see for example equations 9.16 of [5] or 9.29 of [8]). The magnetic field is purely azimuthal: the field lines are circles centered on the dipolar axis. The electric field has no azimuthal component, and the field lines lie in planes which contain the  $z$  axis. (There is cylindrical symmetry about the dipole direction, and we can think of the electric field lines as lying on surfaces of rotation about the  $z$  axis.) Figure 1 shows the electric field vectors and the electric field intensity at  $\omega t = 1$ , the time of transition from the creation of field loops which fade away to creation of loops which propagate out to infinity. The coordinates used are  $\rho = r \sin \theta$ ,  $z = r \cos \theta$ .

Field lines are defined by their tangent being parallel to the field:  $d\mathbf{s} \sim \mathbf{E}$  where  $d\mathbf{s}$  is an increment of length along the field line. Thus  $\frac{dr}{E_r} = \frac{r d\theta}{E_\theta}$  on an electric field line. The resulting differential equation is separable:

$$\begin{aligned} \frac{2d\theta}{\tan \theta} &= \frac{dX}{X} \frac{C(1 - X^2) + XS}{C + XS} \\ [X = kr, \quad C = \cos(X - \omega t), \quad S = \sin(X - \omega t)]. \end{aligned} \quad (3)$$

Integration is elementary since the left-hand side is equal to the differential of  $\ln \sin^2 \theta$  and the right-hand side is equal to the differential of  $\ln[X/(C + XS)]$ . Thus electric field lines are given by

$$\begin{aligned} \sin^2 \theta(r, t) &= \sigma \frac{X}{C + XS} \\ &= \sigma \frac{kr}{\cos(kr - \omega t) + kr \sin(kr - \omega t)}. \end{aligned} \quad (4)$$

The parameter  $\sigma$  is constant for any particular field line (in three dimensions: on its surface of rotation). Equation (4) for the field lines is equivalent to equation (14.46) of Lorrain and Corson [4], and the same as equation (6) of Good [7]. Another way of obtaining the field lines is via the level curves of Zangwill's function  $R(\rho, z)$  ([11], section 20.5.2, with  $\rho$  the distance from the  $z$  axis).

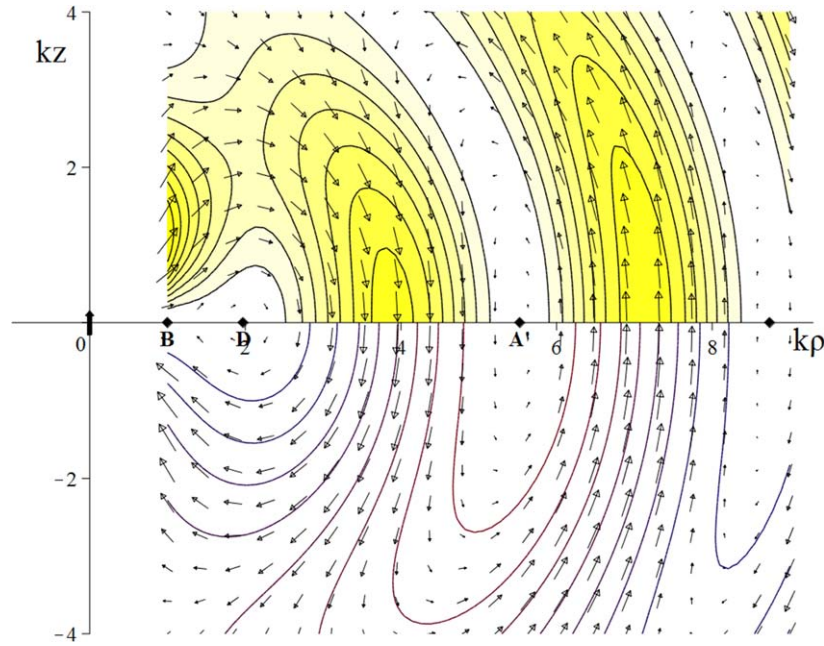


**Figure 1.** Electric field vectors (arrows), electric intensity  $E_r^2 + E_\theta^2$  (contours and shading, upper part of diagram), and electric field lines (lower part of diagram), of electric dipole radiation at  $\omega t = 1$ . The immediate neighborhood of the dipole at the origin has been omitted because the field is so intense as to swamp the outlying regions, even though we have scaled the field components by the factor  $r$  for improved visibility. The diamonds locate the field zeros, labeled as in figure 2.

Field lines cannot cross or merge or recombine except where the vector field amplitude is zero, since for finite field amplitude the line direction  $\mathbf{E}/|\mathbf{E}|$  is well defined. So we next look at the locus of the *zeros of the electric field*. The zeros of interest in the birth of radiation occur in the equatorial plane of the dipole ( $\theta = \pi/2$ ). From (1) we see that in the equatorial plane the radial component  $E_r$  is zero, and that  $E_\theta$  is also zero at the points (circles, in the three-dimensional picture) where  $C(1 - X^2) + XS = 0$ . This condition is equivalent to  $\tan(X - \omega t_0) = X - X^{-1}$ , or to

$$\omega t_0 = k\rho - \arctan(k\rho - 1/k\rho) \pmod{\pi}. \tag{5}$$

We have written  $\rho$  rather than  $r$  to emphasize that the zeros occur in the equatorial plane. Equation (5) is equivalent to (39) of Derby and Olbert [10].

Figure 2 shows two of the branches of equation (5) within one half-cycle,  $0 \leq \omega t \leq \pi$ . At  $t = 0$  the electric field zero nearest the origin is at  $k\rho \approx 4.48$  (point A). At time  $t_c$  given by  $\omega t_c = \sqrt{2} - \arctan(1/\sqrt{2}) \approx 0.7987$  the zero C appears at  $k\rho = \sqrt{2}$  (this point is noted in section 3.3 of [10], and is discussed further below). As time increases from  $t_c$  the zero C bifurcates to the zeros labeled B, D, which move respectively toward and away from the dipole. In the time interval  $t = 0$  to  $t = 1/\omega$  the zero A has moved to A'. The positions of B, D and A' are shown at  $\omega t = 1$ , the transition moment. Another transition moment occurs half a cycle later, when the field directions are reversed.

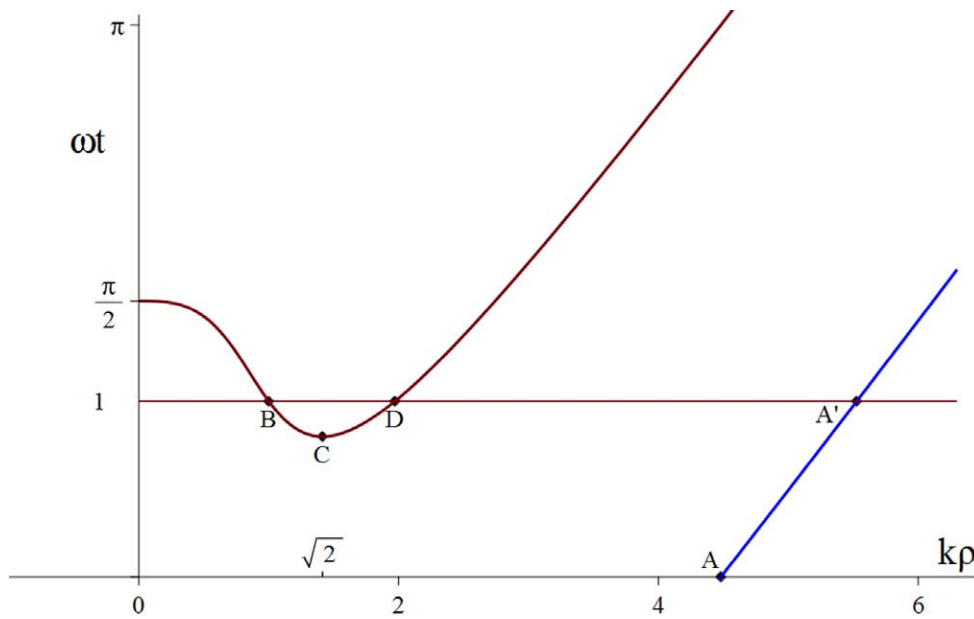


**Figure 2.** Locus of the equatorial plane zeros of the electric field, as a function of time. At any given time there is an infinity of zeros. From  $t = 0$  to  $\omega t_c \approx 0.7987$  the zero nearest the origin is on the curve  $AA'$ . At time  $t_c$  the zero  $C$  appears at  $k\rho = \sqrt{2}$ ; this zero bifurcates as time increases to  $t = 1/\omega$  to the zeros labeled  $B, D$ . In the same time interval  $0 \leq t \leq \omega^{-1}$  the zero  $A$  has moved to  $A'$ . The horizontal line is drawn at  $\omega t = 1$ . The point  $B$  at  $z = 0, k\rho = 1, \omega t = 1$  locates in space and time the transition between closed field loops which *fade away* (with detachment points on  $BC$ ), to loops which *propagate to infinity*. The latter have field line reconnection on the curve joining  $k\rho = 1, \omega t = \pi/2$  to  $B$ .

The point  $C$  is special, because (in the cycle beginning at  $t = 0$ ), for times earlier than  $t_c$  there are no electric field zeros close to the dipole, and at  $t_c$  one zero appears at  $C$ , to immediately split into two zeros moving respectively inward and outward. The location of  $C$  is where  $d(\omega t_0)/d(k\rho) = 0$ , which from equation (5) occurs at

$$k\rho_c = \sqrt{2}, \quad \omega t_c = \sqrt{2} - \arctan(1/\sqrt{2}) \approx 0.7987. \tag{6}$$

Figure 3 shows electric field lines at times  $t = 0.99t_c, t_c, 1.01t_c$ . We see that at these times the field lines are still bound to the dipole charges, but pass through a cusp form at  $\rho_c, t_c$ . In this plot and in figure 4 the field lines indicate the direction of the electric field, not its strength. If we were to make the line thickness proportional to the field strength, the thickness would decrease as the cusp is approached and vanish at the point  $\rho = \rho_c, z = 0$ .

The formation of closed electric field loops begins at  $t = t_c$ , but these loops fade away as time progresses, until  $\omega t > 1$ , as we shall see. From then on till  $\omega t = \pi/2$  we have real radiation, with field loops which propagate to infinity. In the transition from *bound* to *free* fields (those with field lines originating and ending on charges, and those closing on themselves) the field lines contract towards a neck and touch, at which point a bound loop reconnects or bifurcates to a bound loop plus a closed free line. Exactly at this space-time point the field lines cross. This can only happen when the field is zero. So the criterion for the

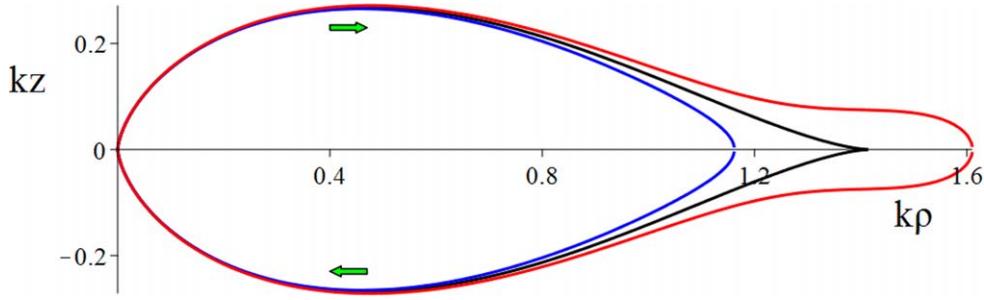


**Figure 3.** Electric field lines in the neighborhood of  $t = t_c$ , drawn according to (4) using  $\sigma = \sigma_c = 2/\sqrt{3}$  (see text, below equation (12)). The cusp line at  $t = t_c$  terminates at the point  $C$  in figure 2 ( $k\rho_c = \sqrt{2}$ ), where the field is zero. It is drawn in black. The other two field lines are drawn at  $t = 0.99t_c$  (red), and at  $t = 1.01t_c$  (blue). The arrows indicate electric field directions, for the three neighboring field lines. At the point of the cusp the field is zero, and the field direction reverses.

formation of loops is that, in the immediate neighborhood of the point  $r = r_0$ ,  $\theta = \frac{\pi}{2}$ ,  $t = t_0$  (a circle in three dimensions) two field lines cross at a field zero. From (4) and (5) we have

$$\begin{aligned} \sin^2 \theta(r_0, t_0) &= 1 \\ &= \sigma_0 \frac{kr_0}{\cos(kr_0 - \omega t_0) + kr_b \sin(kr_0 - \omega t_0)} \end{aligned} \quad (7)$$

$$\omega t_0 = kr_0 - \arctan(kr_0 - 1/kr_0). \quad (8)$$

These two conditions determine possible values of the constant  $\sigma_0$ :

$$\sigma_0 = \pm \frac{1 \pm |X^2 - 1|}{\sqrt{X^4 - X^2 + 1}} \quad (X = kr_0). \quad (9)$$

To find the slopes of the crossing field lines it is convenient to work in cylindrical coordinates. From the field line definition,  $d\rho/E_\rho = dz/E_z$ . At a singular point where the field components are both zero, the slopes  $dz/d\rho$  at an intersection of field lines may be found as in section 3.1 of Derby and Olbert [10], by expanding about the singular point:

$$\frac{dz}{d\rho} = \frac{d\rho \partial_\rho E_z + dz \partial_z E_z}{d\rho \partial_\rho E_\rho + dz \partial_z E_\rho} = \frac{\partial_\rho E_z + (dz/d\rho) \partial_z E_z}{\partial_\rho E_\rho + (dz/d\rho) \partial_z E_\rho}. \quad (10)$$

This is a quadratic for the unknown  $dz/d\rho$ . For dipole radiation the partial derivatives  $\partial_\rho E_\rho$  and  $\partial_z E_z$  are both zero in the equatorial plane  $z = 0$ , and evaluation of the other derivatives gives

$$\frac{dz}{d\rho} = \pm \sqrt{\frac{\partial_\rho E_z}{\partial_z E_\rho}} = \pm \sqrt{1 - (k\rho)^2/2}. \quad (11)$$

This gives zero slope at the cusp point  $k\rho_c = \sqrt{2}$ , as seen in figure 3. For  $k\rho > \sqrt{2}$  the slopes are imaginary: there is no crossing of field lines and no field loops closing on themselves. At

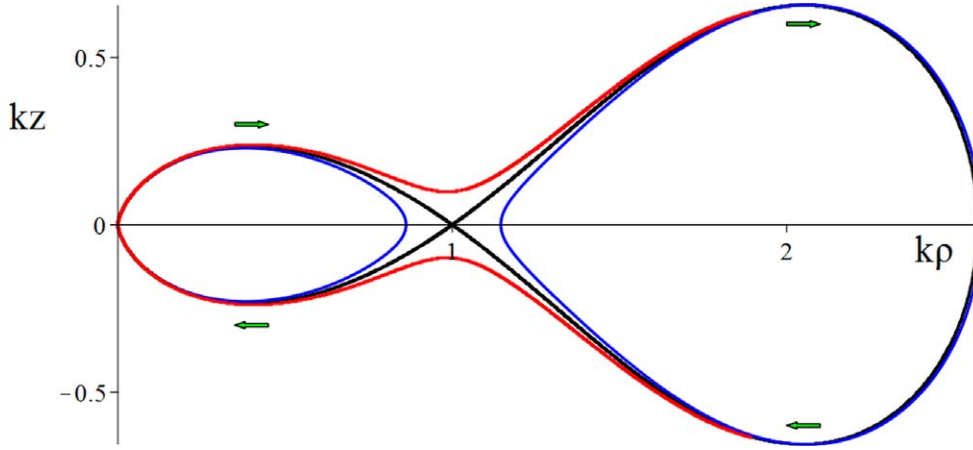


**Figure 4.** Time evolution of electric field lines in the neighborhood of the transition from evanescent to propagating radiation:  $\sigma = 1$ ,  $\omega t = 1$  (point B in figure 2). The  $\sigma$  value corresponds to  $kr_0 = 1$  in (9). The lines are drawn at  $\omega t = 1$  (black), one percent below (red), and one percent above (blue). The arrows indicate electric field directions, for three neighboring field lines. At the birth point  $k\rho = 1$ ,  $z = 0$ ,  $\omega t = 1$  the field is zero, and the field direction changes on the upper part of the figure of eight from inclination at about  $-35^\circ$  (at left) to inclination at  $+35^\circ$  to the  $z = 0$  plane, coinciding with the  $k\rho$  axis in the figure. The closed field loop at the right travels outward as time increases but thins progressively, as explained by (12).

$k\rho = 1$  the crossing field lines are inclined at angles  $\pm \arctan(1/\sqrt{2}) \approx 35^\circ$  to the equatorial plane.

The asymptotic form of equation (4) places a constraint on the value of  $|\sigma_0|$  in equation (9): we have

$$\begin{aligned} \sin^2 \theta(r, t) &= \sigma \frac{kr}{\cos(kr - \omega t) + kr \sin(kr - \omega t)} \\ &\rightarrow \frac{\sigma}{\sin(kr - \omega t)} \quad (kr \gg 1). \end{aligned} \quad (12)$$

Hence radiation fields must originate in field lines which have  $|\sigma_0| < 1$ . Those with  $|\sigma_0| \geq 1$  cannot propagate to infinity. This selects the minus sign in the numerator of (9),  $|\sigma_0| = (1 - |X^2 - 1|)/\sqrt{X^4 - X^2 + 1}$  for radiating fields. However, fields forming loops which die away can have  $|\sigma_0| = (1 + |X^2 - 1|)/\sqrt{X^4 - X^2 + 1}$ , up to the limiting value  $X = \sqrt{2}$ , which gives  $|\sigma_0| = 2/\sqrt{3} \approx 1.1547$  (used in figure 3). These statements are in accord with the observations of Good [7], whose  $K$  corresponds to our  $\sigma$ . He writes ‘It is interesting that for  $1 < |K| < 1.15$ , field lines form loops which break away but eventually dwindle and vanish; whereas for smaller  $|K|$  the loops break away and grow, and for larger  $|K|$  no loops break away’. Lorrain and Corson had previously identified the beginning of radiation at  $|\sigma| = 1$  ([4], p 608).

Figure 4 shows electric field lines at times  $\omega t = 0.99, 1, 1.01$ , drawn with  $\sigma = 2/\sqrt{3}$ . This value of  $\omega t$  corresponds closely to Zangwill’s birth time  $t_Z \approx 0.159T$  ( $T = 2\pi/\omega$ ), or  $\omega t_Z \approx 0.999$ . We see that at the earlier time the field line is still bound to the dipole charges,

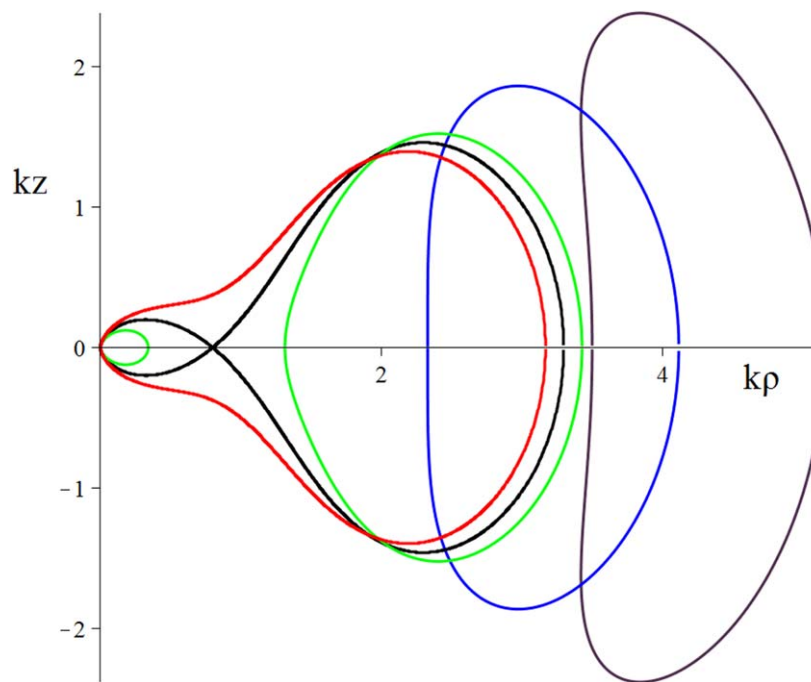


**Figure 5.** Detachment of the electric field loop leading to radiation originating at the electric field zero at  $kr_0 = \frac{4}{5}$ ,  $\omega t_0 \approx 1.22$ , as given by (8), to the left of the point  $B$  in figure 2. The field lines are drawn at  $t_0$  (black),  $0.9t_0$  (red), and  $1.1t_0$  (green), and then at  $\omega t = 2$  and at  $\omega t = 3$  (blue and violet, respectively). These snapshots show the time development of the green just-detached loop drawn at  $t = 1.1t_0$ . The small loop at left draws back to the dipole source, at the origin. The larger loop moves off to the right, growing as it goes.

at the later time the free field line has separated. The closed loop on the right propagates outward, but eventually fades away because  $\sigma = 2/\sqrt{3} > 1$ , as explained above.

Figure 5 shows field line detachment in the radiation interval  $1 < \omega t \leq \pi/2$ . The detached field loops move away from the dipole source and expand. This radiation travels off to infinity unless intercepted.

We note in conclusion that optical vortices, associated with the zeros of complex solutions of the Helmholtz equation, can undergo similar topological reconnection phenomena [18–21]. There the phase of a complex scalar field (from which vector solutions of Maxwell’s equations are found) is undefined at the zeros of the scalar field. As in the birth of radiation, the changes can be large for small changes of parameter.

## Acknowledgments

It is a pleasure to thank David Griffiths and Rufus Boyack for very helpful comments and questions, which have transformed this note. Critical comments by the referees have improved the presentation, and are acknowledged with thanks.

**ORCID iDs**

John Lekner  <https://orcid.org/0000-0003-4675-9242>

**References**

- [1] Hertz H 1900 *Electric Waves (Being Researches on the Propagation of Electric Action with Finite Velocity Through Space)* [2 ed, English translation by D E Jones; 1 ed 1894] 2nd edn (London: Macmillan) Figures 27–30
- [2] Bitter F 1956 *Currents, Fields and Particles* (New York: MIT and Wiley) Figure 8.19
- [3] Jones D S 1964 *The Theory of Electromagnetism* (Oxford: Pergamon)
- [4] Lorrain P and Corson D R 1970 *Electromagnetic Fields and Waves* 2nd edn (San Francisco, CA: Freeman) Figure 14-9
- [5] Jackson J D 1975 *Classical Electrodynamics* 2nd edn (New York: Wiley)
- [6] Reitz J R, Milford F J and Christy R W 1980 *Foundations of Electromagnetic Theory* (Reading, MA: Addison-Wesley) Figure 20-3
- [7] Good R H 1981 Dipole radiation: a film *Am. J. Phys.* **49** 185–7
- [8] Griffiths D 1981 *Introduction to Electrodynamics* (Englewood Cliffs, NJ: Prentice-Hall)
- [9] Ohanian H C 1988 *Classical Electrodynamics* (Boston, MA: Allyn and Bacon) Figure 14.5
- [10] Derby N and Olbert S 2008 Electromagnetic fields of a linear antenna *Am. J. Phys.* **76** 1048–53
- [11] Zangwill A 2013 *Modern Electrodynamics* (Cambridge: Cambridge University Press) Figures 20.5–6
- [12] Olbert S, Belcher J and Price R H 2012 The creation and propagation of radiation *Am. J. Phys.* **80** 321–8
- [13] Slepian J 1951 Lines of force in electric and magnetic fields *Am. J. Phys.* **19** 87–90
- [14] Hamilton J C and Schwartz J L 1971 Electric fields of moving charges: a series of four film loops *Am. J. Phys.* **39** 1540–2
- [15] Tsien R Y 1972 Pictures of dynamic electric fields *Am. J. Phys.* **40** 46–56
- [16] Belcher J W and Olbert S 2003 Field line motion in electromagnetism *Am. J. Phys.* **71** 220–8
- [17] Wolf A, Van Hook S J and Weeks E R 1996 Electric field line diagrams don't work *Am. J. Phys.* **64** 714–24
- [18] Berry M V and Dennis M R 2007 Topological events on wave dislocation lines: birth and death of loops, and reconnection *J. Phys. A: Math. Gen.* **40** 65–74
- [19] Berry M V and Dennis M R 2012 Reconnections of wave vortex lines *Eur. J. Phys.* **33** 723–31
- [20] Nye J F 2016 Events in fields of optical vortices: rings and reconnection *J. Opt.* **18** 105602
- [21] Andrejic P and Lekner J 2017 Topology of phase and polarization singularities in focal regions *J. Opt.* **19** 105609